Evidence for non-self-similarity and transitional increment of scaled energy in the 2005 west off Fukuoka seismic sequence

Seung-Hoon Yoo,[1] Junkee Rhie,[1] Hoseon Choi,[1,2] and Kevin Mayeda[3]

Received 26 November 2009; revised 8 March 2010; accepted 14 April 2010; published 20 August 2010.

[1] We investigated seismic scaling relations of the 2005 west off Fukuoka seismic sequence in Japan using a coda-based methodology. Two independent methods such as coda source spectrum method and coda spectral ratio method were applied to seismic waveform data recorded at four broadband seismic stations located around the epicenter of the mainshock. The corner frequencies determined from both methods are consistent with each other, and the scaling relations between the corner frequencies and the corresponding seismic moments are clearly non-self-similar in both cases. Moreover, the scaled energy obtained from the coda source spectrum method shows that there is a transitional change in the scaled energy with seismic moment. The scaled energy is larger for events with Mw >5.0 than for events with Mw <4.0. For events larger than Mw 5.0, the scaled energy is almost constant and it means that they obey self-similar scaling. For events smaller than about Mw 4.0, the scaled energy is more or less constant, but it is difficult to decide whether it follows self-similar or non-self-similar scaling because of scatter and the limitation of the minimum moment magnitude (Mw 3.4). The most important observation is a linear increment of the scaled energy between about Mw 4.0 and 5.0. These observations imply that the rupture dynamics for larger and smaller earthquakes are different and that the change in dynamics may occur continuously between about Mw 4.0 and 5.0 in this seismic sequence.

Citation: Yoo, S.-H., J. Rhie, H. Choi, and K. Mayeda (2010), Evidence for non-self-similarity and transitional increment of scaled energy in the 2005 west off Fukuoka seismic sequence, *J. Geophys. Res.*, *115*, B08308, doi:10.1029/2009JB007169.

1. Introduction

[2] Understanding the dynamics of faulting is one of the key issues in earthquake source physics. Even though many researchers have been trying to resolve the problem using many different methods, our knowledge of earthquake dynamics is still very poor. One way to study earthquake dynamics is to use the seismic scaling relations of dynamic source parameters, such as corner frequency (f_c) and scaled energy ($\tilde{e} = E_R/M_0$) versus static measures of earthquake size such as seismic moment (M_0). The seismic scaling can show whether dynamics of different-sized earthquakes are the same. It is widely accepted that the static measure of earthquake size is well established. However, the dynamic parameters are more difficult to determine, and even the same data set can provide different results depending on the method used.

[3] For many years, self-similar seismic scaling, $M_0 \sim f_c^{-3}$ or $M_0 \sim E_R$, has been popular in the earthquake physics society [*Aki*, 1967; *Kanamori and Anderson*, 1975], and it is still supported by many researchers [e.g., *McGarr*, 1999; *Ide and Beroza*, 2001; *Ide et al.*, 2003; *Prieto et al.*, 2004]. On the contrary, sufficient compelling evidence for non-self-similarity of earthquakes has been reported for more than a decade [e.g., *Kanamori et al.*, 1993; *Abercrombie*, 1995; *Mayeda and Walter*, 1996; *Izutani and Kanamori*, 2001; *Mori et al.*, 2003]. The main point of debate is whether the measured dynamic parameters are reliable, because they can be easily contaminated by complex propagation, attenuation, site, and source radiation effects. Since those effects can significantly distort estimates of source parameters even in a good recording environment such as a deep borehole [*Ide et al.*, 2003], great care is required to correct for those effects. To circumvent these problems, coda waves can be used because they inherently average out the unnecessary propagation and source radiation effects [*Aki and Chouet*, 1975; *Rautian and Khalturin*, 1978; *Mayeda and Walter*, 1996]. Therefore, several methods have been developed to measure source parameters using coda waves and adequate corrections for path and site effects [e.g., *Mayeda et al.*, 2003; *Mayeda and Walter*, 1996; *Morasca et al.*, 2005a]. The seismic sequence consisting of many earthquakes with similar focal mechanisms and close hypocenters provides good data sets because those earthquakes are likely to occur in similar seismogenic con-

[1] School of Earth and Environmental Science, Seoul National University, Seoul, South Korea.
[2] Korea Institute of Nuclear Safety, Daejeon, South Korea.
[3] Weston Geophysical Corporation, Lexington, Massachusetts, USA.

Copyright 2010 by the American Geophysical Union.
0148-0227/10/2009JB007169

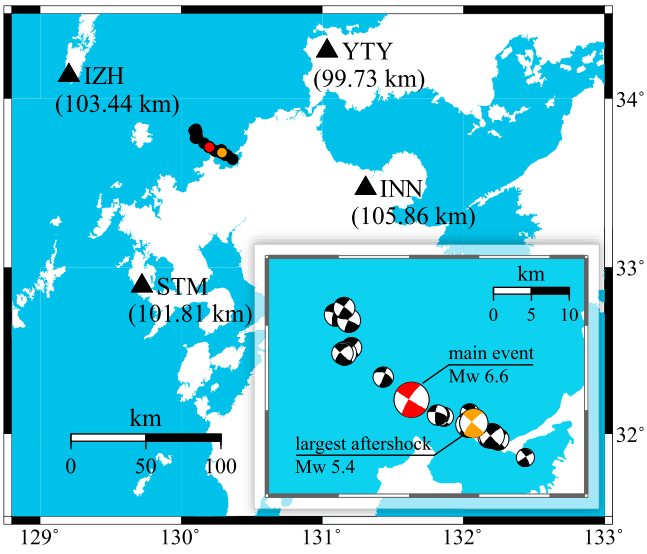

Figure 1. Location map of 20 earthquakes for the west off Fukuoka seismic sequence and the four stations used in this study. Red, orange, and black circles indicate the main event, the largest aftershock, and other aftershocks, respectively. Four F-net broadband stations are indicated by black triangles. The numbers in parentheses represent the epicentral distance from the main event. Inset shows the focal mechanisms of the sequence.

ditions. In this study, we applied the stable coda-based methods to a well-recorded seismic sequence in Japan.

2. Data

[4] The west off Fukuoka earthquake (M_{JMA} 7.0) occurred at 0153:40 UTC on 20 March 2005. This event is the first M7-class intraplate earthquake in the northern Kyushu region recorded by F-net, the broadband seismic network operated by the National Institute for Earth Science and Disaster Prevention [*Matsumoto et al.*, 2006]. We selected the mainshock and 19 aftershocks ranging between Mw 3.4 and 6.6 (Table 1 and Figure 1). The epicenters and the origin times of the sequence were determined by Hi-net using the AQUA (Accurate and Quick Analysis) system (http://www.hinet.bosai.go.jp), and their seismic moments were estimated by F-net from long-period regional waveform modeling (http://www.fnet.bosai.go.jp). The focal mechanisms of the main event and aftershocks are very similar and show a left-lateral strike-slip movement on a fault plane with a strike of N122°E. The epicenters of the aftershocks are aligned bilaterally on the fault plane, and the centroid depths of all events are within the range of 5–17 km. The waveforms recorded at four broadband stations (INN, IZH, STM, and YTY) with good azimuthal coverage and similar epicentral distances (99.73–105.86 km) from the mainshock were used.

3. Methods

[5] We used two independent coda-based methods, namely, the coda source spectrum method and the coda spectral ratio method, to derive the scaling relations for the Fukuoka sequence. The first method provides stable moment rate spectra of local and regional events using empirical corrections for source-to-coda transfer function and path and site effects. From calibrated moment rate spectra, we can estimate several dynamic source parameters such as corner frequency, radiated energy, and apparent stress. Since the details of the method are described in many previous studies [e.g., *Mayeda and Walter*, 1996; *Mayeda et al.*, 2003; *Mayeda et al.*, 2005; *Morasca et al.*, 2005a], we briefly describe our data processing in the next section. The second method is the coda spectral ratio method, which can determine the corner frequencies of source spectra without any assumption of path and site effects by using two closely located events sharing common path and site effects [*Mayeda et al.*, 2007]. In this study, we are interested in the scaling relations of corner frequency and scaled energy versus seismic moment. First, we obtained corner frequencies of the sequence data from the coda source spectrum

Table 1. Source Parameters for Events Used in This Study[a]

Event	Latitude (°N)	Longitude (°E)	Depth (km)	Mw	f_c^1 (Hz)	f_c^2 [b] (Hz)	Scaled Energy E_R/M_o
200503200153	33.712	130.203	11.0	6.6	0.1504 (±0.0036)	0.1534 (±0.0161)	5.66E−5 (±4.33E−6)
200503200532	33.813	130.095	8.0	4.4	0.9813 (±0.0363)	0.9772	8.92E−6 (±9.42E−7)
200503200843	33.696	130.286	14.0	3.6	2.2144 (±0.1846)	2.0184	8.92E−6 (±1.62E−6)
200503201052	33.806	130.114	5.0	4.5	0.8771 (±0.0540)	0.6966	1.60E−5 (±2.43E−6)
200503201108	33.821	130.107	17.0	4.1	1.4925 (±0.2008)	1.4125	1.36E−5 (±2.73E−6)
200503201138	33.717	130.198	8.0	4.4	0.9789 (±0.0324)	1.0233	1.08E−5 (±6.06E−7)
200503202117	33.712	130.203	11.0	3.9	2.0160 (±0.1393)	1.7783	1.64E−5 (±2.52E−6)
200503210637	33.774	130.118	8.0	4.0	1.7783 (±0.0612)	1.6788	1.45E−5 (±7.70E−7)
200503211459	33.767	130.108	8.0	4.5	0.9600 (±0.0112)	0.7674	1.97E−5 (±1.27E−6)
200503241438	33.739	130.163	8.0	3.9	2.4167 (±0.1749)	2.7479	2.22E−5 (±2.97E−6)
200503241843	33.694	130.240	5.0	3.9	1.1996 (±0.1403)	1.1749	6.06E−6 (±5.85E−7)
200503251203	33.767	130.105	8.0	4.1	1.5991 (±0.1134)	1.7865	1.56E−5 (±1.27E−6)
200504011252	33.665	130.327	8.0	4.1	1.1954 (±0.0409)	1.1402	8.22E−6 (±7.95E−7)
200504052259	33.692	130.249	8.0	3.7	1.8362 (±0.1463)	2.7164	9.54E−6 (±6.87E−7)
200504192111	33.684	130.292	8.0	5.4	0.5254 (±0.0357)	0.5356 (±0.0216)	4.56E−5 (±6.00E−6)
200504192122	33.683	130.292	11.0	4.5	1.2494 (±0.1110)	1.2461 (±0.0404)	3.35E−5 (±3.67E−6)
200504192144	33.668	130.314	8.0	4.3	1.1910 (±0.1037)	1.2086 (±0.1455)	1.81E−5 (±2.75E−6)
200504200009	33.682	130.284	8.0	4.8	1.0104 (±0.0035)	1.0928 (±0.1954)	4.26E−5 (±9.04E−7)
200504271843	33.643	130.365	8.0	3.4	3.1737 (±0.2772)	2.9139 (±0.3832)	1.16E−5 (±2.19E−6)
200505011623	33.669	130.318	8.0	4.7	0.8756 (±0.0123)	0.7379	2.35E−5 (±4.44E−7)

[a]The variable f_c^1 is corner frequency from coda source spectrum method; f_c^2 is corner frequency from coda spectral ratio method.
[b]Average and standard deviation are calculated when the number of available data is at least two.

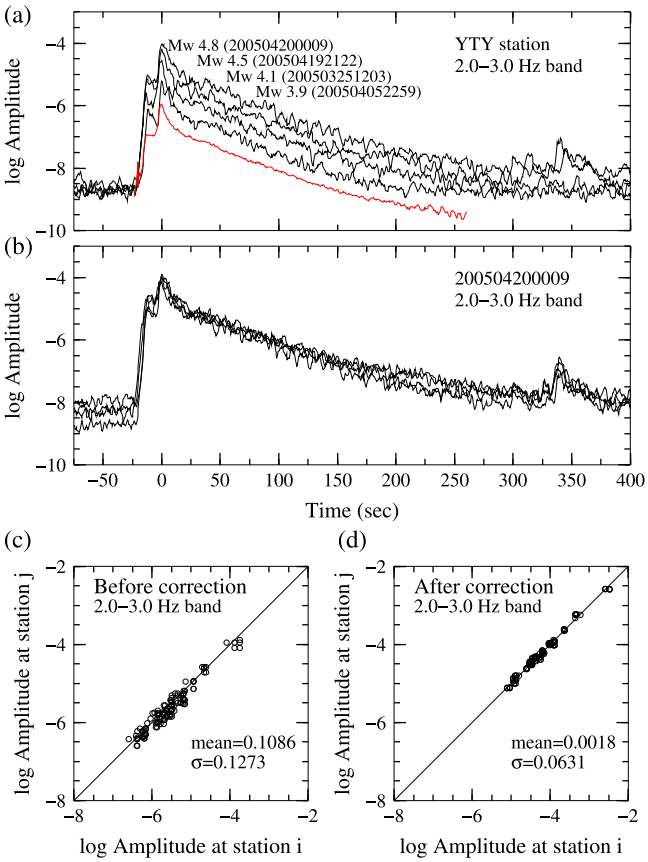

Figure 2. (a) Narrow-band coda envelopes of events observed at YTY station at 2.0–3.0 Hz. The levels are different, but the shapes of the coda envelopes are almost identical. For presentation purposes, the amplitude of the reference envelope (red) is modified. (b) Narrow-band coda envelopes of the event 200504200009 (Mw 4.8) for all stations at 2.0–3.0 Hz. They show small variations in amplitude. It indicates that they share similar path and site effects. (c) Plots of interstation scatter of uncorrected coda amplitudes at 2.0–3.0 Hz for common events. Here all possible combinations of station pairs are used. (d) Same as Figure 2c for corrected amplitudes. The mean and standard deviation for corrected amplitudes are smaller than those for uncorrected amplitudes.

method and derived the scaling relation of corner frequency versus seismic moment. Second, we determined the same scaling relationship from the coda spectral ratio method and then compared both methods' results. The comparison shows that both relationships are nearly identical, and it indicates that calibrated moment rate spectra obtained from the coda source spectrum method are quite reliable. Finally, we computed radiated energy from calibrated moment rate spectra and constructed the scaling relation of scaled energy versus seismic moment. The following briefly outlines the processes for two methods.

3.1. Coda Source Spectrum Method

3.1.1. Preprocesses and Corrections for Path and Site Effects

[6] We processed two horizontal component waveforms by deconvolving the instrument response to velocities and applying a four poles and two passes butterworth filter for 12 narrow-frequency bands ranging between 0.05 and 8.0 Hz and then calculated the narrow-band coda envelopes by taking $\log_{10}$ of two horizontal envelopes and averaging them at each center frequency. By doing this, we can effectively minimize the source radiation effects. To measure the nondimensional coda amplitude, a reference coda envelope for each frequency is necessary. Our target events are clustered with a maximum event separation of only 31.33 km, and the coda envelope shapes of all events are nearly identical at each station (Figures 2a and 2b). This indicates that all envelopes recorded at each station share the source radiation and propagation effects at a given frequency band. Therefore, we constructed the reference coda envelope for each station and frequency by averaging normalized coda envelopes of all events after the alignment of main peaks [*Hartse et al.*, 1995]. The maximum length of the time window of the coda envelope was determined on the basis of the signal-to-noise ratio and the arrival times of main peaks of the following events [*Mayeda et al.*, 2003]. To remove the effects due to the misalignment of the observed and reference coda envelopes, we allowed the small amount of time shift using cross-correlation. After time shift, we measured nondimensional coda amplitudes by DC shifting the reference envelope to fit the observed envelopes using an L-1 norm. The differences in measured coda amplitudes among stations are smaller than other results from previous studies [e.g., *Morasca et al.*, 2005a, 2005b]. To remove the remaining uncorrected path effects, we applied an empirical correction method known as the Extended Street and Herrmann Correction, which is described in the work of *Mayeda et al.* [2003]. After path correction, we found that corrected amplitudes of given stations have similar patterns for all events. Thus we further corrected the relative site effects by minimizing amplitude differences among stations for all events. The path and site corrections reduce the interstation scatter on average by a factor of 3 for all frequency bands. Figures 2c and 2d show the interstation scatter of the uncorrected and corrected amplitudes for all events at 2.0–3.0 Hz frequency band.

3.1.2. Grid Search Method to Find the Best Source-to-Coda Transfer Function

[7] Since we have independent estimates of seismic moments for all events from long period waveform analysis, we can compute the theoretical source spectra if we have a proper scaling relation for the corner frequencies. To do that, we used the magnitude distance and amplitude correction (MDAC) algorithm of *Walter and Taylor* [2001]. This algorithm allows for the variation of the corner frequency that does not have to be self-similar. To find the best source-to-coda transfer function, we applied a grid search technique for the apparent stress of the reference event (σ_a') and the scaling parameter (ε). The theoretical scaling relation of the apparent stresses with different seismic moments is

$$\sigma_a = \sigma_a' \left(\frac{M_0}{M_0'}\right)^{\psi}, \text{where } \psi = \frac{\varepsilon}{\varepsilon + 3}, \tag{1}$$

where σ_a is the apparent stress of the target event [*Wyss*, 1970], (σ_a') and (M_0') are the apparent stress and seismic moment of the reference event, and ε is the scaling

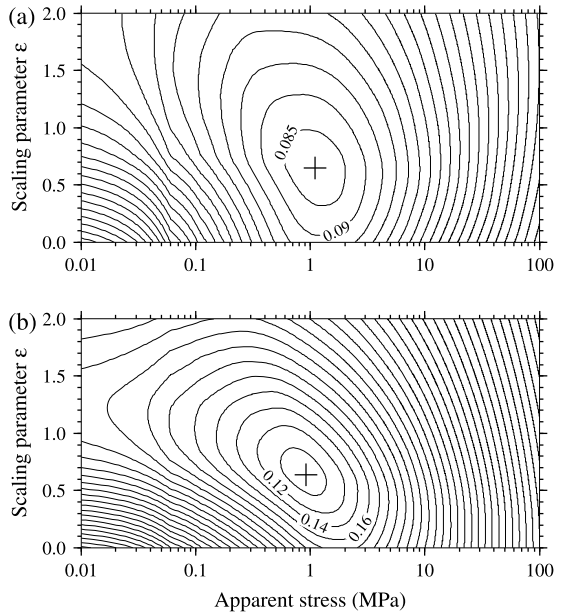

Figure 3. The results of a grid search for apparent stress and scaling parameter. Crosses indicate the best fitting point for (a) the coda source spectrum method and (b) the coda spectral ratio method.

parameter. In this study, we took the main event as the reference event. For all events, theoretical source spectra were computed using the MDAC algorithm for given apparent stress and scale parameter. Source-to-coda transfer function was computed by DC shifting the corrected amplitudes to fit theoretical source spectra for all events at each frequency. The best apparent stress and scaling parameter provide the minimum misfit between theoretical spectra and calibrated coda amplitudes for all frequencies. Figure 3a shows the contour plot of the grid search, which has an obvious global minimum of error at apparent stress of 1.09 MPa and a scaling parameter of 0.65. By doing this, we obtained the coda-derived moment rate spectra for all events simultaneously. The individual seismic moment and corner frequency of each station and event were estimated by finding the best fit *Brune*'s [1970] theoretical spectrum using a grid search. The average values of four stations were taken as the final estimate for each earthquake. Moment magnitudes estimated from the moment rate spectra are consistent with those from time domain waveform inversion (Figure 4).

3.1.3. Estimation of Radiated Energy

[8] The scaled energy is defined as the ratio of the total radiated energy to seismic moment, and it is an important parameter in understanding the dynamic properties of the earthquake [*Aki*, 1966; *Wyss*, 1970]. To investigate the variation in the scaled energy with increasing seismic moment, we need to estimate the total radiated energy of the earthquake. By using the coda-derived moment rate spectrum, we calculated the *S* wave radiated energy as follows:

$$E_S = \frac{I}{4\pi^2\rho\beta^5}\int_0^\infty |\omega \cdot \dot{M}(\omega)|^2 d\omega, \qquad (2)$$

where I is the RMS radiation pattern for S wave, and it is known as 2/5. The density (ρ) and the S wave velocity (β) are set to be 2700 kg/m^3 and 3.5 km/s, respectively [*Mayeda and Walter*, 1996].

[9] *Ide and Beroza* [2001] pointed out that the limited bandwidth on energy estimation can lead to a substantial underestimate or can introduce an artificial upper bound of the radiated seismic energy. To avoid this problem, appropriate compensations are needed to calculate radiated energy. For the low frequency, we extrapolated the value at the lowest frequency to 0 Hz. For the high frequency, we assumed an ω-square falloff from the frequency at 6–8 Hz band to infinite frequency. To obtain the total radiated energy, we multiplied 1.07 by the calculated radiated energy of S wave to account for the energy radiated by P wave. The behavior of the scaled energy as a function of seismic moment is discussed later.

3.2. Coda Spectral Ratio Method

[10] To verify the scaling relation of corner frequency versus seismic moment obtained from the coda source spectrum method, we recomputed the corner frequencies of the events using the coda spectral ratio method [*Mayeda et al.*, 2007]. In general, spectral ratio methods have a couple of advantages over the methods that are based on moment rate spectra. Since these methods use spectral ratio from closely located events, we can assume that the path and site effects would be canceled and only effects due to the difference in source would be remaining. Moreover, these methods are very easy to apply because complicated corrections for the path and site effects are not necessary. Coda spectral ratio method improves upon the direct wave spectral ratio method because it utilizes the averaging nature of coda waves and is virtually free of source radiation pattern and directivity effects. Recently, *Mayeda et al.*, [2007] showed that the coda wave amplitude ratios observed from closely located events are much more stable than those derived from direct S wave ratios by roughly a factor of 3 to 4.

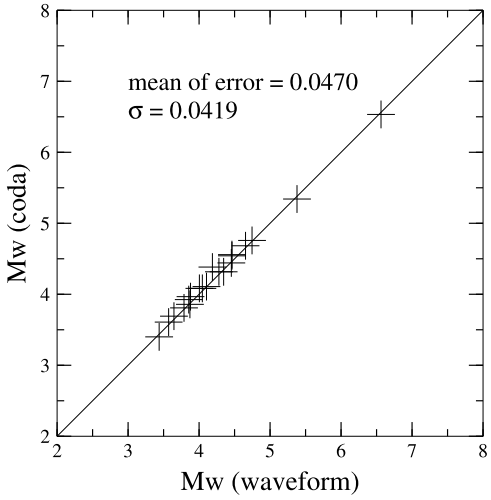

Figure 4. The comparison of Mw from waveform inversion and coda-derived spectra.

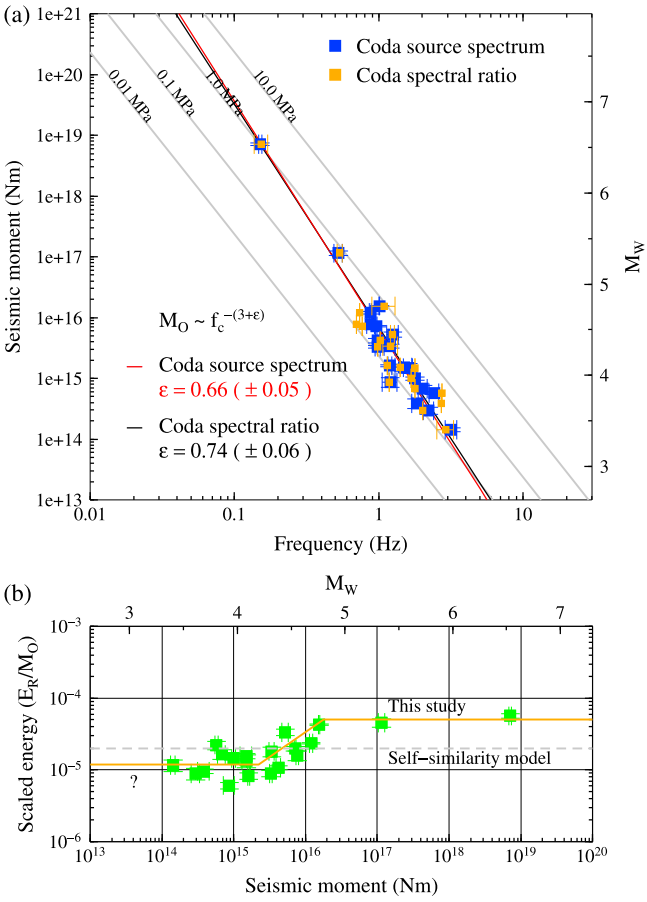

Figure 5. (a) Corner frequency versus seismic moment for the Fukuoka sequence. Blue squares represent the corner frequencies and seismic moments determined from coda source spectrum method. Vertical and horizontal error bars represent 1 standard deviation for four stations. Orange squares represent the results obtained from coda spectral ratio method. Red and black lines indicate the best fit regressions calculated from bootstrap test for blue and orange squares, respectively. For reference, the shaded lines for constant apparent stresses of 0.01, 0.1, 1, and 10 MPa are plotted. (b) Scaled energy versus seismic moment for the sequence. Scaled energy varies with seismic moment, and a linear increment occurs between about Mw 4.0 and 5.0. Vertical and horizontal error bars represent 1 standard deviation for four stations.

[11] Assuming a single corner frequency source model [*Aki*, 1967; *Brune*, 1970], the ratio of the moment rate spectra for two events given by

$$\frac{\dot{M}_1(\omega)}{\dot{M}_2(\omega)} = \frac{M_{0_1}\left[1+(\omega/\omega_{c_2})^2\right]^{p/2}}{M_{0_2}\left[1+(\omega/\omega_{c_1})^2\right]^{p/2}}, \quad (3)$$

where M_0 is the seismic moment, ω_c is the angular corner frequency, and p is the high-frequency decay rate. To compute reliable coda spectral ratios, we need pairs of events with similar locations and their magnitude differences should be large enough to distinguish corner frequencies of the large and small event. In this study, we selected event pairs satisfying the minimum magnitude difference and event separation criteria. We chose a minimum magnitude difference of 0.9 in Mw and the maximum event separation criterion was set to 20 km. Here moment magnitudes obtained from the coda source spectrum method were used for direct comparison. Twenty-five event pairs satisfied the conditions, and the maximum separation was at most ~17 km. We computed a spectral ratio from uncorrected coda amplitudes measured in the previous section and calculated an average spectral ratio for four stations. Only events which were well recorded at all four stations were considered.

[12] We used all event pairs to find the best apparent stress and scaling parameter using a similar grid search technique applied in the coda source spectrum method. The best fitting grid point is 0.91 MPa and 0.64 for the apparent stress and scaling parameter, respectively (Figure 3b). It confirms that both independent methods result in very similar results. For an individual event pair, a grid search technique for the two corner frequencies was applied to find the best fit spectral ratio curve. The results were plotted along with the previous results derived from coda source spectrum method in Figure 5a.

4. Results and Discussion

[13] Under the self-similar scaling suggested by *Kanamori and Anderson* [1975] and *Hanks* [1977], seismic moment (M_0) and corresponding corner frequency (f_c) must satisfy the simple relation $M_0 \propto f_c^{-3}$. However, *Kanamori and Rivera* [2004] suggested a non–self-similar relationship between seismic moment and corner frequency $M_0 \propto f_c^{-(3+\varepsilon)}$, where ε represents the deviation from self-similarity and should be a small positive number. The results from both methods show that non-self-similar scaling can better explain observed corner frequency versus seismic moment relations. To estimate the possible error of the obtained scaling parameter due to event selection, we utilized the bootstrap test. We randomly selected 13 of 19 aftershocks and calculated the best fit scaling parameter in a least squares sense. Here we constrained that the regression line should pass through the estimate of the mainshock corner frequency. The averages and 1 standard deviation of the scaling parameter estimated from 1000 realizations are $\varepsilon = 0.66 \pm 0.05$ for the coda source spectrum method and $\varepsilon = 0.74 \pm 0.06$ for the coda spectral ratio method (see Figure 5a). These values are consistent with results obtained from all events (see Figure 3).

[14] As mentioned previously, the scaling parameter can be used to investigate the difference in rupture dynamics of different-sized earthquakes. In addition, it can play an important role in assessing the seismic hazard. Although the self-similar scaling relation, $\varepsilon = 0$, has been widely used for strong ground motion simulations [e.g., *Irikura*, 1983; *Frankel*, 1995; *Zeng et al.*, 1994], *Malagnini et al.* [2008] demonstrated that strong non-self-similarity, $\varepsilon = 1.7 \pm 0.3$, is required to explain the characteristics of strong ground motion recordings in the entire central Apennines region. This result indicates that the estimate of the scaling parameter is quite important to assess a more realistic and reliable seismic hazard, especially for the specific regions where self-similar scaling is not applicable.

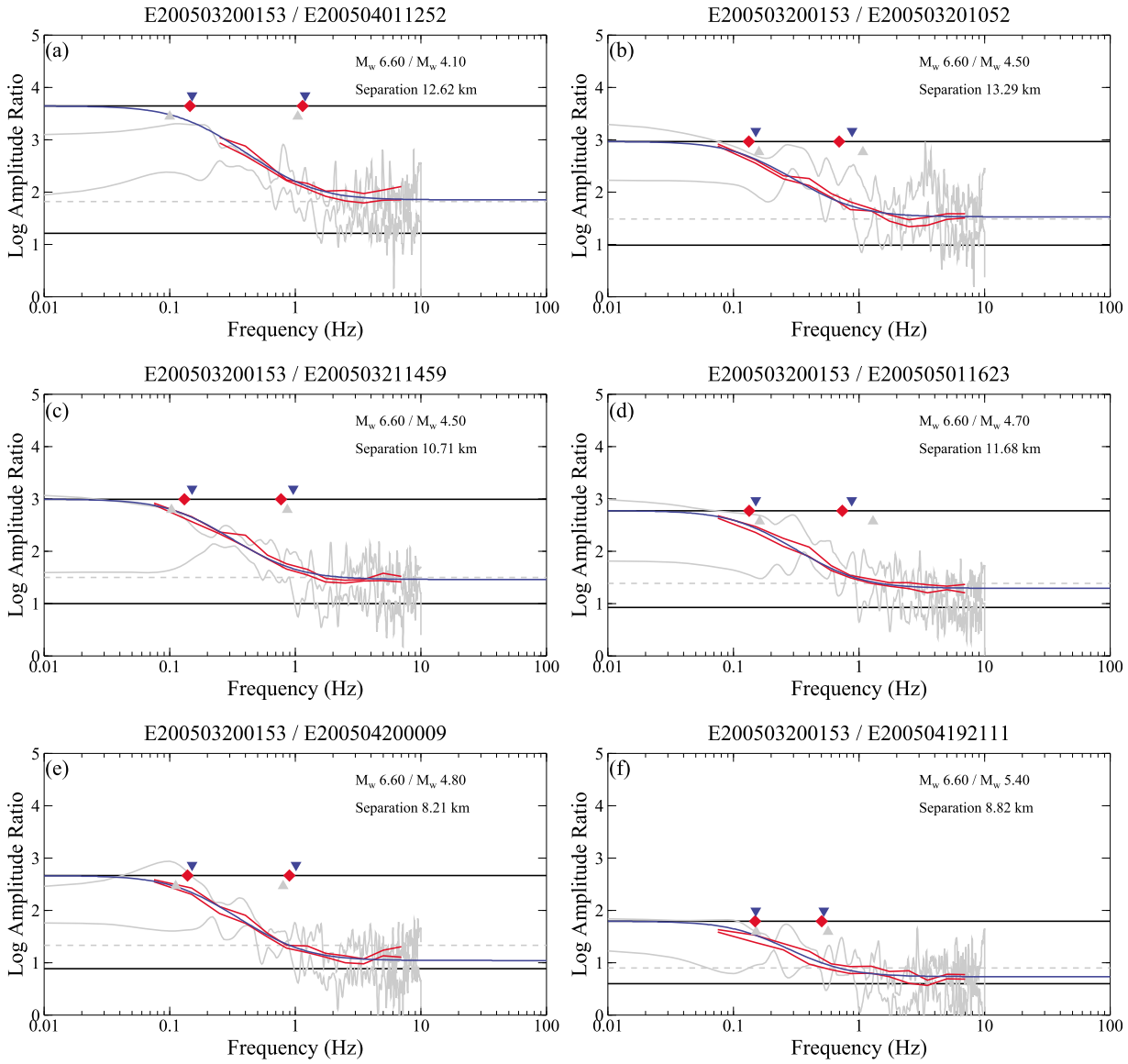

Figure 6. Examples of the spectral ratio curves for coda waves (red lines) and direct *P* waves (shaded lines). Two red and shaded lines indicate ±1 standard deviation of averaged ratios for four stations. Blue inverted triangles, red diamonds, and shaded triangles represent estimated corner frequencies from coda source spectrum, coda spectral ratio, spectral ratio of direct *P* wave, respectively. Upper and lower black horizontal lines indicate low- and high-frequency asymptotes predicted by the self-similar ω-square source model by *Brune* [1970] (P = 2), respectively. Dashed shaded lines indicate high-frequency asymptotes with high-frequency decay rate P = 1.5.

[15] The scaling relationship for the same seismic sequence was studied by *Tajima and Tajima* [2007] using direct *P* wave spectral ratios. They analyzed 13 events recorded at the same F-net stations used in this study and concluded that the Fukuoka sequence is likely to obey self-similarity. This contradictory result mainly comes from the estimates of the corner frequencies for the small events. It is well known that the *P* wave has only 4%–10% of the *S* wave energy with some uncertainty [e.g., *Boatwright and Fletcher*, 1984]. Moreover, the amplitudes of *P* waves are sensitive to heterogeneity, rupture directivity, and source radiation. Therefore, the reliability of the corner frequency estimates using direct *P* waves, especially for small events, can only be guaranteed if a network that has many stations with good azimuthal coverage is used [e.g., *Izutani*, 2005; *Prieto et al*, 2004]. On the other hand, coda methods are relatively free from various unwanted effects and can provide more reliable results, even though the number of stations used is small [e.g., *Hartse et al.*, 1995; *Mayeda et al.*, 2003, 2007]. Although *Tajima and Tajima*'s [2007] data set is not the same as ours, we tried to reproduce their result using our dataset. The estimated corner frequencies using direct *P* waves are not much different from the results using coda waves (see Figure 6). However, we found that the corner frequency scatter for direct *P* waves from station to station is almost three times larger than those for coda waves. In addition, the

estimates of the corner frequencies for small events provided by *Tajima and Tajima* 2007 show more scatter than our results obtained using coda methods. It may indicate that a small difference in data selection can lead to completely different results when less stable direct waves are used.

[16] Our results agree well with several previous results obtained from the coda source spectrum method for regional events in the Lunigiana-Garfagnana region in the northern Apennines, Italy [*Morasca et al.*, 2005b], and from the coda spectral ratio method for the Hector Mine seismic sequence in southern California [*Mayeda et al.*, 2007], the 2002 San Guiliano seismic sequence in southern Italy [*Malagnini and Mayeda*, 2008], and the Colfiorito seismic sequence in central Italy [*Malagnini et al.*, 2008]. In addition, *Izutani* [2005] also found a similar scaling relationship for the 2004 mid-Niigata earthquake and its four aftershocks using direct wave spectral ratios.

[17] In detail, it is obvious that the f_c^{-3} scaling is not applicable for the whole sequence. However, for the events larger than Mw ~5.0, it is likely that self-similar scaling can better explain the observation (Figure 5a). It indicates that there is a transitional change in the scaling relationship with the size of earthquakes. This result is consistent with the recent observation for the Chi-Chi, Taiwan, sequence [*Mayeda and Malagnini*, 2009].

[18] The scaling relation of scaled energy versus seismic moment derived from the coda source spectrum method shows more interesting features. Figure 5b shows the relationship between the seismic moment and scaled energy, and we can see the transitional behavior more clearly. The scaled energy increases linearly with increasing seismic moment between about Mw 4.0 and Mw 5.0, whereas for the events larger than Mw 5.0 or smaller than 4.0, the scaled energy seems to be more or less constant. Although it is unclear whether the scaled energy would be constant or decrease monotonically at even lower seismic moment because our dataset is limited at Mw 3.4, our observation clearly shows that the large earthquakes over Mw ~5.0 have different rupture dynamic properties from the small earthquakes below Mw 4.0 and the changes occur between Mw 4.0 and 5.0. The moment range associated with the change in dynamic properties might vary with tectonic settings and/or the status of faults. But still much more evidence would be necessary to make a more definitive conclusion.

5. Conclusions

[19] We investigated the seismic scaling of the 2005 west off Fukuoka sequence using two separate coda-based techniques. The scaling relation of the corner frequency and the seismic moment obtained from the coda source spectrum method is the same as the relation derived from the coda spectral ratio method, which does not require path and site corrections. Both methods result in non-self-similar scaling with a scale parameter of about $\varepsilon = 0.7$. This indicates that the path and site corrections for the coda source spectrum method are reliable.

[20] The spectral ratio curves for the mainshock and selected aftershocks clearly show the change in scaling relations (see Figure 6). The self-similar ω-square models cannot match the observed spectral ratio curves at high frequencies when spectral ratios are computed for the mainshock and small aftershocks (Mw <4.70) (Figures 6a–6d). However, the spectral ratio curves for the mainshock and large aftershocks (Mw ~5.0) show good agreement with the self-similar model (Figures 6e and 6f).

[21] The trend of the scaled energy as a function of the seismic moment shows more interesting features. We found that relatively larger earthquakes (Mw >5.0) obey self-similarity, which is consistent with the observation from the spectral ratio curves. The smaller earthquakes (Mw <4.0) are likely to follow self-similarity, too, but it is inconclusive because of the scatter and limited minimum seismic moment of our dataset. Although smaller and larger earthquake groups have more or less constant scaled energy, the scaled energy for larger earthquakes is much larger than that for smaller events. In between those two groups, we found that the scaled energy is gradually increasing. This observation may imply that the change in rupture dynamics, such as fluid pressurization [*Kanamori and Heaton*, 2000], continuously occurs in a given moment range and makes large earthquakes different from small ones in terms of their rupture dynamics and the efficiency of seismic energy radiation.

[22] **Acknowledgments.** We thank the operators of F-net for making their data publicly available. This work was funded by the Korean Meteorological Administration and Development Program under grant CATER 2008-5113. K. Mayeda was supported by Weston Geophysical subcontract GC19762NGD and AFRL contract FA8718-06-C-0024.

References

Abercrombie, R. E. (1995), Earthquake source scaling relationships from −1 to 5 ML using seismograms recorded at 2.5-km depth, *J. Geophys. Res.*, *100*(B12), 24,015–24,036, doi:10.1029/95JB02397.

Aki, K. (1966), Generation and propagation of G waves from the Niigata earthquake of June 16, 1964. Part 2: Estimation of earthquake moment, from the G wave spectrum, *Bull. Earthquake Res. Inst. Univ. Tokyo*, *44*, 73–88.

Aki, K. (1967), Scaling law of seismic spectrum, *J. Geophys. Res.*, *72*(4), 1217–1231, doi:10.1029/JZ072i004p01217.

Aki, K., and B. Chouet (1975), Origin of coda waves: Source, attenuation and scattering effects, *J. Geophys. Res.*, *80*(23) 3322–3342, doi:10.1029/JB080i023p03322.

Boatwright, J., and J. Fletcher (1984), The partition of radiated energy between P and S waves, *Bull. Seismol. Soc. Am.*, *74*, 361–376.

Brune, J. N. (1970), Tectonic stress and spectra of seismic shear waves from earthquakes, *J. Geophys. Res.*, *75*(26) 4997–5009, doi:10.1029/JB075i026p04997. (Correction, *J. Geophys. Res.*, *76*, 5002, 1971.)

Frankel, A. (1995), Simulating strong ground motions of large earthquakes using recordings of small earthquakes: The Loma Prieta mainshock as a test case, *Bull. Seismol. Soc. Am.*, *85*, 1144–1160.

Hanks, T. C. (1977), Earthquake stress drops, ambient tectonic stresses and stresses that drive plate motions, *Pure Appl. Geophys.*, *115*, 441–458.

Hartse, H. E., W. S. Phillips, M. C. Fehler, and L. S. House (1995), Single-station spectral discrimination using coda waves, *Bull. Seismol. Soc. Am.*, *85*, 1464–1474.

Ide, S., and G. C. Beroza (2001), Does apparent stress vary with earthquake size?, *Geophys. Res. Lett.*, *28*(17), 3349–3352, doi:10.1029/2001GL013106.

Ide, S., G. C. Beroza, S. G. Prejean, and W. L. Ellsworth (2003), Apparent break in earthquake scaling due to path and site effects in deep borehole recordings, *J. Geophys. Res.*, *108*(B5), 2271, doi:10.1029/2001JB001617.

Irikura, K. (1983), Semi-empirical estimation of strong ground motions during large earthquakes, *Bull. Disaster Prev. Res. Inst. Kyoto Univ.*, *33*, 63–104.

Izutani, Y. (2005), Radiated energy from the mid Niigata, Japan, earthquake of October 23, 2004, and its aftershocks, *Geophys. Res. Lett.*, *32*, L21313, doi:10.1029/2005GL024116.

Izutani, Y., and H. Kanamori (2001), Scale-dependence of seismic energy-to-moment ratio for strike-slip earthquakes in Japan, *Geophys. Res. Lett.*, *28*(20), 4007–4010, doi:10.1029/2001GL013402.

Kanamori, H. K., and D. L. Anderson (1975), Theoretical basis of some empirical relations in seismology, *Bull. Seismol. Soc. Am.*, *65*, 1073–1095.

Kanamori, H., and T. H. Heaton (2000), Microscopic and macroscopic physics of earthquakes, in *Geocomplexity and the Physics of Earthquakes*, *Geophys. Monogr. Ser.*, vol. 120, edited by J. B. Rundle et al., pp. 147–163, AGU, Washington, D. C.

Kanamori, H., and L. Rivera (2004), Static and dynamic scaling relations for earthquakes and their implications for rupture speed and stress drop, *Bull. Seismol. Soc. Am.*, *94*, 314–319.

Kanamori, H., E. Hauksson, L. K. Hutton, and L. M. Jones (1993), Determination of earthquake energy release and ML using TERRAscope, *Bull. Seismol. Soc Am.*, *83*, 330–346.

Malagnini, L., and K. Mayeda (2008), High-stress strike-slip faults in the Apennines: An example from the 2002 San Giuliano earthquakes (southern Italy), *Geophys. Res. Lett.*, *35*, L12302, doi:10.1029/2008GL034024.

Malagnini, L., L. Scognamiglio, A. Mercuri, A. Akinci, and K. Mayeda (2008), Strong evidence for non-similar earthquake source scaling in central Italy, *Geophys. Res. Lett.*, *35*, L17303, doi:10.1029/2008GL034310.

Matsumoto, T., Y. Ito, H. Matsubayashi, and S. Sekiguchi (2006), Spatial distribution of F-net moment tensors for the 2005 west off Fukuoka Prefecture earthquake determined by the extended method of the NIED F-net routine, *Earth Planets Space*, *58*, 63–67.

Mayeda, K., and L. Malagnini (2009), Apparent stress and corner frequency variations in the 1999 Taiwan (Chi-Chi) sequence: Evidence for a step-wise increase at Mw ~5.5, *Geophys. Res. Lett.*, *36*, L10308, doi:10.1029/2009GL037421.

Mayeda, K., and W. R. Walter (1996), Moment, energy, stress drop, and source spectra of western United States earthquakes from regional coda envelopes, *J. Geophys. Res.*, *101*(B5), 11,195–11,208, doi:10.1029/96JB00112.

Mayeda, K., A. Hofstetter, J. L. O'Boyle, and W. R. Walter (2003), Stable and transportable regional magnitudes based on coda-derived moment rate spectra, *Bull. Seismol. Soc. Am.*, *93*, 224–239.

Mayeda, K., R. Gök, W. R. Walter, A. Hofstetter (2005), Evidence for non-constant energy/moment scaling from coda-derived source spectra, *Geophys. Res. Lett.*, *32*, L10306, doi:10.1029/2005GL022405.

Mayeda, K., L. Malagnini, and W. R. Walter (2007), A new spectral ratio method using narrow band coda envelopes: Evidence for non-self-similarity in the Hector Mine sequence, *Geophys. Res. Lett.*, *34*, L11303, doi:10.1029/2007GL030041.

McGarr, A. (1999), On relating apparent stress to the stress causing earthquake fault slip, *J. Geophys. Res.*, *104*(B2), 3003–3011, doi:10.1029/1998JB900083.

Morasca, P., K. Mayeda, L. Malagnini, and W. R. Walter (2005a), Coda-derived source spectra, moment magnitudes and energy-moment scaling in the western Alps, *Geophys. J. Int.*, *160*, 263–275.

Morasca, P., K. Mayeda, R. Gök, L. Malagnini, and C. Eva (2005b), A break in self-similarity in the Lunigiana-Garfagnana region (northern Apennines), *Geophys. Res. Lett.*, *32*, L22301, doi:10.1029/2005GL024443.

Mori, J., R. E. Abercrombie, and H. Kanamori (2003), Stress drops and radiated energies of aftershocks of the 1994 Northridge, California, earthquake, *J. Geophys. Res.*, *108*(B11), 2545, doi:10.1029/2001JB000474.

Prieto, G. A., P. M. Shearer, F. L. Vernon, and D. Kilb (2004), Earthquake source scaling and self-similarity estimation from stacking P and S spectra, *J. Geophys. Res.*, *109*, B08310, doi:10.1029/2004JB003084.

Rautian, T. G., and V. I. Khalturin (1978), The use of coda for determination of the earthquake source spectrum, *Bull. Seismol. Soc. Am.*, *68*, 923–948.

Tajima, R., and F. Tajima (2007), Seismic scaling relations and aftershocks activity from the sequences of the 2004 mid Niigata and the 2005 west off Fukuoka earthquakes (Mw 6.6) in Japan, *J. Geophys. Res.*, *112*, B10302, doi:10.1029/2007JB004941.

Walter, W. R., and S. R. Taylor (2001), A revised magnitude and distance amplitude correction (MDAC2) procedure for regional seismic discriminants: Theory and testing at NTS, *Rep. UCRL-ID-146882*, Lawrence Livermore Natl. Lab., Livermore, Calif., 21 Dec. (Available at http://www.llnl.gov/tid/lof/documents/pdf/240563.pdf)

Wyss, M. (1970), Stress estimates of South American shallow and deep earthquakes, *J. Geophys. Res.*, *75*(8), 1529–1544, doi:10.1029/JB075i008p01529.

Zeng, Y., J. G. Anderson, and G. Yu (1994), A composite source model for computing realistic synthetic strong ground motions, *Geophys. Res. Lett.*, *21*(8), 725–728, doi:10.1029/94GL00367.

H. Choi, Korea Institute of Nuclear Safety, 34 Gwahak-ro, Yuseong-gu, Daejeon 305-338, South Korea.

K. Mayeda, Weston Geophysical Corporation, 181 Bedford St., Ste. 1, Lexington, MA 02420, USA.

J. Rhie and S.-H. Yoo, School of Earth and Environmental Science, Seoul National University, 599 Gwanak-ro, Gwanak-gu, Seoul, 151-742, South Korea. (rhie@snu.ac.kr)